

Robust Multi-Sensor Fusion for Perception in Harsh Weather Conditions

Adrian Dziuba¹, Feliks Karpiński¹ and Henryk Kasprzak^{1,*}

¹ Faculty of Information and Communication Technology, Wrocław University of Science and Technology, Wrocław, 50-371, Poland

*Corresponding author: henryk.ka@pwr.edu.pl

Abstract. It is still necessary to enhance autonomous driving and other intelligent robots' perceptive reliability in inclement weather. The performance of cameras, LiDAR, and radar sensors will be diminished by environmental conditions like rain, fog, and light variations, which will result in increased noise, observational gaps, and decreased recognition accuracy. This work proposes a novel adaptive Bayesian multi-sensor fusion algorithm that can automatically modify fusion weights in real time and adjust the weights of various sensors in response to environmental changes. The stability of perception will be enhanced by a novel structure based on uncertainty propagation and probability theory. For the experiment, four common unfavourable weather conditions—light rain, heavy rain, dense fog, and sun glare—were chosen for both a simulation and an actual driving environment. According to the aforementioned findings, under all test circumstances, the adaptive fusion approach has been demonstrated to increase the perception accuracy of classical static fusion by at least 7%. Furthermore, the system's error rate and perception failure incidence are more than 50% lower than those of single-sensor and deep learning-based baselines. The findings show that real-time uncertainty estimation and the dynamic and irregular nature of disturbances are the two primary causes of the challenge in dealing with environmental changes. This research proposes a system that can successfully handle the ongoing issues of all-weather autonomous driving perception while exhibiting strong stability both on average and under challenging conditions.

Keywords: *Sensor Fusion, Adverse Weather, Autonomous Vehicles, Bayesian Methods*

Received on 23 March 2025, Accepted on 19 August 2025, Published on 27 August 2025

Copyright © 2025 Author(s), licensed to JAAT. This is an open access article distributed under the terms of the CC BY-NC-SA 4.0, which permits copying, redistributing, remixing, transformation, and building upon the material in any medium so long as the original work is properly cited.

Introduction

The second is that intelligent robots and self-driving cars have a very difficult time receiving strong signals during inclement weather. Rain, snow, and fog are examples of environmental variables that will enhance camera, LiDAR, and radar noise, occlusion, and signal deterioration. The safety and stability of autonomous cars in challenging outdoor conditions will be at risk due to the aforementioned issues, which will lead to a failure of object detection and scene identification [1]. Many empirical investigations conducted recently have demonstrated that particular sensor types are unsuitable for field robotics or real-world driving applications because they are unable to deliver steady perception in a variety of weather situations [2].

Because of the aforementioned factors, numerous research teams have been working on multi-sensor fusion, utilising the distinct kinds and capabilities of multiple sensors [3]. In order to manage sensor noise and extract integrated features from multi-modal data, traditional fusion solutions have been built around probabilistic data association techniques, Kalman and particle filter-based frameworks, and Bayesian inference models [4]. Adaptive and scalable perception algorithms that incorporate high-dimensional sensor data and lessen the effects of inclement weather have been developed thanks to advancements in deep learning and probabilistic graphical models [5]. The majority of current systems lack theoretical resilience guarantees under extreme conditions, lack explicit uncertainty quantification, or have not been able to adaptively modify fusion algorithms in response to rapid declines in sensor performance [6]. The primary issues with real-time autonomous systems are static weighting, weak cross-condition validation, and restricted error propagation modelling [7].

This research proposes a new robust multi-sensor fusion technique for resilient perception in bad weather. The suggested approach uses Bayesian probabilistic models to disperse uncertainty during fusion and ascertain the true dependability of sensors. Theoretically, a new performance measure appropriate for assessing systems in various weather circumstances has been established, and all-weather robustness tests for propagating faults have been conducted. The suggested technique has been found to be dependable and general in situations without clear weather based on several experiments using both synthetic and real data. This paper is organised as follows: The probabilistic modelling of sensors and weather-induced uncertainty is introduced in Section 2. The mathematical formulation, theoretical analysis, and architectural schematic of the aforementioned algorithm are presented in Section 3. After presenting the experimental setup and findings, Section 4 performs a methodical analysis. The study's findings and recommendations for further research are presented in Section 5.

Theoretical Foundations

Probabilistic Sensor Models

For a high-performance multiple-sensor perception system, first model the characteristics and noise of each observer during the observation process. For instance, cameras' outputs are typically modelled as being contaminated by Gaussian or Poisson noise distributed according to calibration experiment findings since they are frequently impacted by photometric noise, optical distortion, and changes in ambient light [8]. LiDAR sensors are 3D point cloud sensors, and the signal-to-noise ratio of the measured signal decreases with increasing distance or air interference. Although range-dependent Gaussian models are frequently used, their shortcomings when noise variances fluctuate are somewhat noticeable [9]. Compound noise models that take into account both additive and multiplicative uncertainty must be used since radar sensors are vulnerable to distinctive speckle noise and Doppler-related artefacts, despite their relative robustness against some optical issues [10].

Sensor modelling is further obscured by unfavourable weather. When combined, rain, fog, and snow result in attenuation, a decreased effective range, and an increase in outliers, necessitating adaptive probabilistic treatment. The measurement distribution may deviate from the conventional Gaussian assumption if raindrops cover the camera lens [11]. Fog causes bias in LiDAR returns and decreases point cloud density, necessitating the use of weather-sensitive, spatially variable noise models [12]. When heavy rain is present, radar is susceptible to clutter and non-stationary noise; dynamic statistical models that can adjust to changes in signal properties over time are appropriate for this issue [13].

Numerous academics have recently put forth adaptable and context-aware probability models. Static, weather-agnostic assumptions are less reliable than methods based on Gaussian mixture models, scene-aware noise estimation, and spatial and environmental parameter adaptability [14]. Based on the aforementioned, we explicitly represent sensor uncertainties as model parameters that change based on the environment [15].

Uncertainty and Error Analysis

In inclement weather, a variety of factors, including environmental and physical elements as well as system issues, can lead to sensor mistakes. In optical sensors, water droplets and fog particles result in both random occlusions and systematic attenuation, which increases noise and lowers measurement accuracy [16]. Range estimate and object boundary recognition will be erroneous if LiDAR signals scatter in the presence of rain or snow, as this could lead to missing or erroneous returns [17]. When dynamic clutter from reflected precipitation is added, radar inaccuracy grows nonlinearly, increasing both the output variance and the probability of false alarms [18].

Quantification of uncertainty aids in assessing the reliability of perception. As measures of the dispersion or uncertainty in sensor data, entropy and variance are commonly employed [19]. The aforementioned empirical research indicates that the distribution of signals shifts from unimodal to long-tailed or even bimodal forms when the degree of fog or rain increases [20]. If you ignore the pattern of shifting uncertainty, risk will be significantly underestimated and the safe fallback mode or decision threshold won't be activated.

There are issues with the model both now and in the future. In order to calculate sensor dependability in real time, adaptive entropy and variance estimates are introduced to the pre-processing pipeline of the sensor data. It serves as a foundation for the subsequent fusion algorithms that can actively modify the weight of fusion and error propagation by using uncertainty information [21].

Bayesian Fusion Frameworks

Bayesian inference is the foundation of the majority of effective multi-sensor fusion techniques for dynamic uncertainty and safety-critical situations. Sensor observations and system states are processed using a random variable model to provide updated posterior belief distributions using Bayes' theorem [22]. This paradigm serves as the foundation for traditional algorithms like the Kalman filter, as well as more sophisticated particle filters and recursive Bayesian estimators for non-linear, non-Gaussian sensor models [23].

The introduction of factor graphs to manage complex connections between sensors and their surroundings in a large-scale and easily expandable way for real-time systems is a common trend in recent years. The aforementioned frameworks facilitate both geographical and temporal data linkage and are appropriate for managing the massive amounts of data in large-scale sensor networks. These days, robustness in a degraded-performance environment for these sensors can be improved by using the dynamic reliability score or adaptive prior, which is based on ongoing monitoring of sensor uncertainty.

In this paper, we construct a multi-level Bayesian fusion framework. Our approach is unique in that we have officially incorporated real-time uncertainty scores into the posterior update step. As a result, during the fusion process, errors propagate uniformly across all layers of the perception stack and measurements are adaptively reweighted. The general approach mentioned above is more stable and capable of managing the altered conditions brought on by inclement weather.

Algorithm Analysis

Mathematical Formulation

To achieve reliable perception in adverse weather, it is essential to rigorously define the measurement processes for all sensor modalities and establish a cohesive probabilistic fusion framework. Let \mathbf{z}_i^t denote the observation from sensor i at time t , and \mathbf{x}^t the environmental state to be estimated—such as object pose or scene map. Each sensor's measurement can be described by the observation model:

$$\mathbf{z}_i^t = h_i(\mathbf{x}^t) + \epsilon_i^t \quad \text{Eq. (1)}$$

where $h_i(\cdot)$ embodies sensor i 's response function, and ϵ_i^t is zero-mean noise, typically modeled as a Gaussian: $\epsilon_i^t \sim \mathcal{N}(0, \Sigma_i^t)$.

Assuming conditional independence across sensors, the joint likelihood of all observations at time t given the state can be factorized as:

$$p(\mathbf{z}^t | \mathbf{x}^t) = \prod_{i=1}^N p(\mathbf{z}_i^t | \mathbf{x}^t) \quad \text{Eq. (2)}$$

where N is the total number of sensor types.

The target is to infer the posterior distribution of the latent state:

$$p(\mathbf{x}^t | \mathbf{z}^{1:t}) \propto p(\mathbf{z}^t | \mathbf{x}^t) p(\mathbf{x}^t | \mathbf{z}^{1:t-1}) \quad \text{Eq. (3)}$$

In practical implementation, Bayesian filtering (such as an extended Kalman filter or a particle filter) recursively estimates this posterior. Each iteration involves prediction-propagating the prior $p(\mathbf{x}^t | \mathbf{z}^{1:t-1})$ via a motion or system model—and update-refining the state estimate via new fused measurements.

Our architecture (see Figure 1) integrates dynamic reliability assessment: sensor noise covariance Σ_i^t adapts to weather-influenced uncertainty, thereby modulating the update step. This formulation allows the fusion center to weigh sensors according to real-time estimated reliability, reducing the influence of degraded modalities and enhancing overall perceptual stability [24].

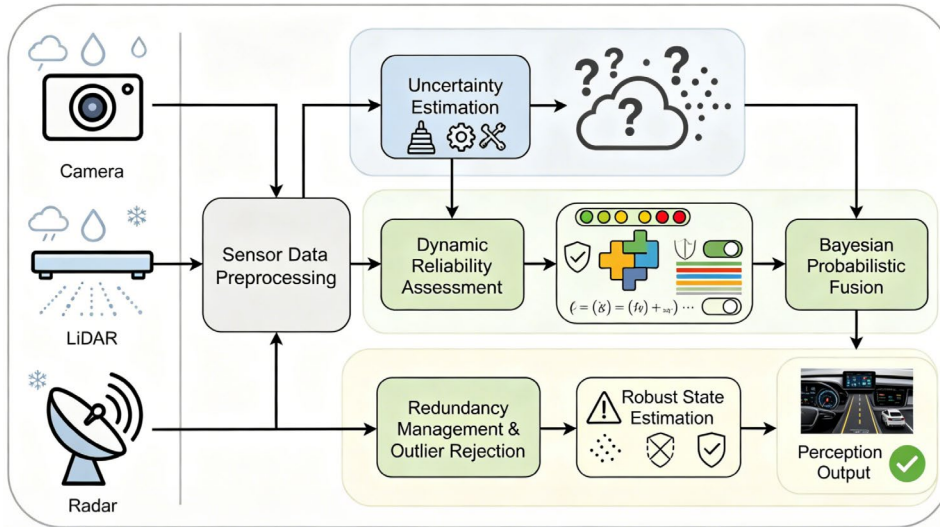


Figure 1. Algorithm Processing Flowchart.

Robustness Evaluation Metrics

Robustness in sensor fusion refers to the algorithm's ability to maintain high perception accuracy despite severe noise, sensor failure, or unexpected environmental changes. To objectively assess this property, we define several quantitative evaluation metrics based on confidence intervals and expected posterior contraction.

A primary robustness indicator is the weighted fusion confidence interval for the estimated state $\hat{\mathbf{x}}^t$, derived as:

$$\mathcal{C}^t = \begin{bmatrix} \hat{\mathbf{x}}^t - \alpha \cdot \sqrt{\text{tr}(\Sigma_{\text{fusion}}^t)} \\ \hat{\mathbf{x}}^t + \alpha \cdot \sqrt{\text{tr}(\Sigma_{\text{fusion}}^t)} \end{bmatrix} \quad \text{Eq. (4)}$$

where $\hat{\mathbf{x}}^t$ is the fused estimate, Σ_{fusion}^t the posterior covariance, and α a confidence scaling factor.

Another important metric is the robustness score (R^t), defined as:

$$R^t = 1 - \frac{\sum_{i=1}^N \text{tr}(\Sigma_i^t \cdot W_i^t)}{\text{tr}(\Sigma_{\text{fusion}}^t)} \quad \text{Eq. (5)}$$

Here, W_i^t is the adaptive fusion weight for each sensor, determined using uncertainty propagation and dynamic reliability scoring.

The probabilistic outlier rejection rate (\mathcal{O}^t) is used to quantify the frequency of detected spurious sensor measurements filtered during fusion:

$$\mathcal{O}^t = \frac{1}{N} \sum_{i=1}^N \mathbb{I}[z_i^t \notin \mathcal{C}^t] \quad \text{Eq. (6)}$$

where $\mathbb{I}[\cdot]$ is the indicator function.

These metrics frame the theoretical basis for evaluating how well the fusion architecture maintains bounded uncertainty and prevents error amplification. Figure 2 depicts the modular architecture, highlighting how each component contributes to the robustness objectives.

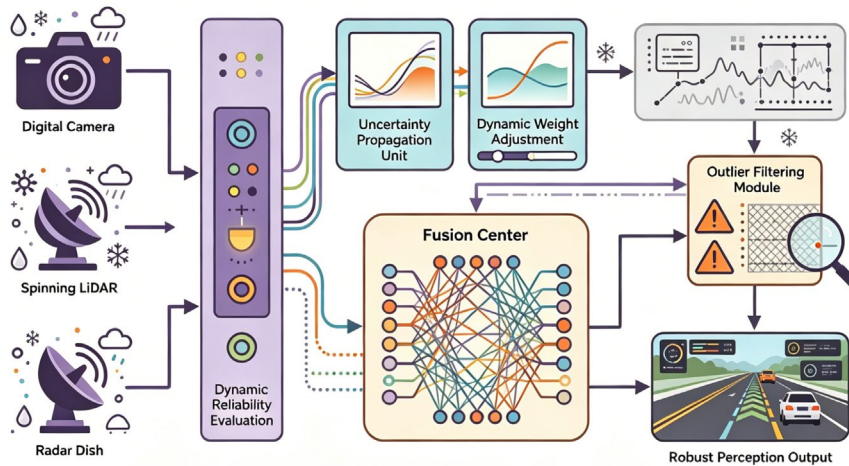


Figure 2. Modular Fusion Architecture Diagram.

By explicitly integrating real-time confidence, dynamic weighting, and outlier filtering, our method ensures resilience across diverse operational scenarios while maintaining interpretable performance guarantees [25].

Error Propagation Study

Understanding how estimation error propagates throughout the sensor fusion pipeline is foundational to assessing the reliability of perception systems in unpredictable environments. The process begins by modeling how the underlying system state transitions over time, accounting for both deterministic dynamics and stochastic disturbances. We represent this evolution as follows: Let the system state at time t evolve according to the function below, where $f(\cdot)$ denotes the process model and ω^t represents process noise:

$$\mathbf{x}^t = f(\mathbf{x}^{t-1}) + \omega^t \quad \text{Eq. (7)}$$

In practice, the expected state prediction at the current time step is calculated by taking the mathematical expectation over the process model:

$$\hat{\mathbf{x}}_{|t-1}^t = \mathbb{E}[f(\mathbf{x}^{t-1})] \quad \text{Eq. (8)}$$

The uncertainty associated with this prediction, formalized as the prior error covariance, advances with the following equation. In it, F^t indicates the Jacobian of the process model with respect to state, and Q^t the covariance of process noise:

$$P_{|t-1}^t = F^t P^{t-1} (F^t)^\top + Q^t \quad \text{Eq. (9)}$$

Upon acquiring new sensory observations, the fusion algorithm integrates these measurements, dynamically adjusting for each sensor's reliability. The Kalman gain, which dictates how new data influence the estimate, is given by:

$$K^t = P_{|t-1}^t (H^t \Sigma^t (H^t)^\top + R^t)^{-1} \quad \text{Eq. (10)}$$

Here, H^t is the Jacobian of the observation model, Σ^t is the fused observation noise covariance, and R^t represents aggregated sensor noise.

The posterior state estimate is then formed by correcting the predicted estimate with the innovation term, incorporating new data as weighted by the Kalman gain:

$$\hat{\mathbf{x}}^t = \hat{\mathbf{x}}_{|t-1}^t + K^t (\mathbf{z}^t - h(\hat{\mathbf{x}}_{|t-1}^t)) \quad \text{Eq. (11)}$$

Correspondingly, the posterior covariance-signifying residual estimation uncertainty after measurement fusion-updates as:

$$P^t = (I - K^t H^t) P_{|t-1}^t \quad \text{Eq. (12)}$$

A central concern for robustness is how these updates modulate uncertainty. If weather conditions degrade one or more sensors, the algorithm inflates related covariance values in R^t , which directly reduces the influence of

noisy modalities on the final estimate. To summarize this effect, we introduce a propagation index representing the contraction (or expansion) of uncertainty through an update step:

$$\Gamma^t = \frac{\text{tr}(P^t)}{\text{tr}(P_{t-1}^t)} \quad \text{Eq. (13)}$$

A value of $\Gamma^t < 1$ suggests that fusion and measurement updates are effectively reducing system uncertainty, which is the hallmark of robust fusion. This progression is depicted conceptually in Figure 3, where the various sources of uncertainty -originating from sensor observations and process dynamics-are traced through each stage of the estimation pipeline. The diagram clarifies how adaptive fusion logic either mitigates or transmits uncertainty based on real-time measurement trustworthiness.

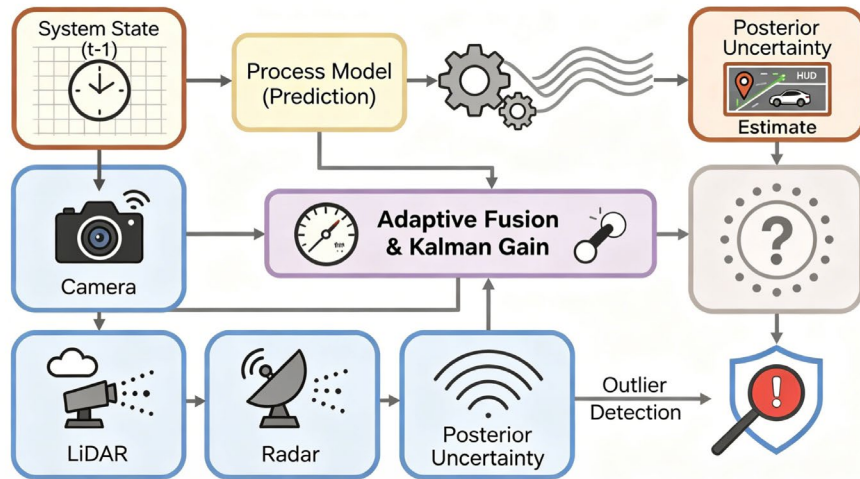


Figure 3. Error Propagation in Adaptive Sensor Fusion.

Simulation, Results, and Discussion

Experimental Design and Setup

To conduct a comprehensive resilience test, four relevant unfavourable weather scenarios were chosen for both high-fidelity models and actual field data in the experiment. A variety of scenarios and sensor installation techniques have been developed to mimic actual autonomous vehicle issues.

Custom weather modules have been added to the simulation platform (CARLA 0.9.13) to accurately replicate low-angle morning glare, heavy rain, dense fog, and moderate rain. At least 45,000 annotated frames were available in each scenario, and over eight significant field events—such as actual precipitation and fog—were added. The sensor array included an automobile FMCW radar (200m range), a 32-beam LiDAR with a 120m range, and a four-RGB camera system (30Hz, 1080p). Attach all sensors firmly to minimise relative motion, and do fine-grained calibration every other week using chequerboard and reflectivity target methods. Time-synchronization was appropriate for cross-modal fusion since it preserved sub-5 ms drift.

The first is data preprocessing, which includes things like boosting contrast and lowering noise. The analysis's integrity was preserved since only data frames with confirmed temporal and spatial congruence across all modalities were retained.

Figure 4 depicts the entire extent of the adverse weather test bed. Here, each subfigure represents a distinct case study. A typical urban simulation during light rain is shown in Figure 4a, where the sensor is only impacted by surface light reflection and vision is still rather excellent. Heavy rain causes quite severe occlusion, as seen in Figure 4b, and both the camera and LiDAR data loss rates significantly rise. Dense fog significantly limits both visibility and range-based detection because it is almost opaque in the far field, as seen in Figure 4c. The early-morning sun glare seen in Figure 4d indicates that the dynamic range and contrast of the image sensor need to be fixed.

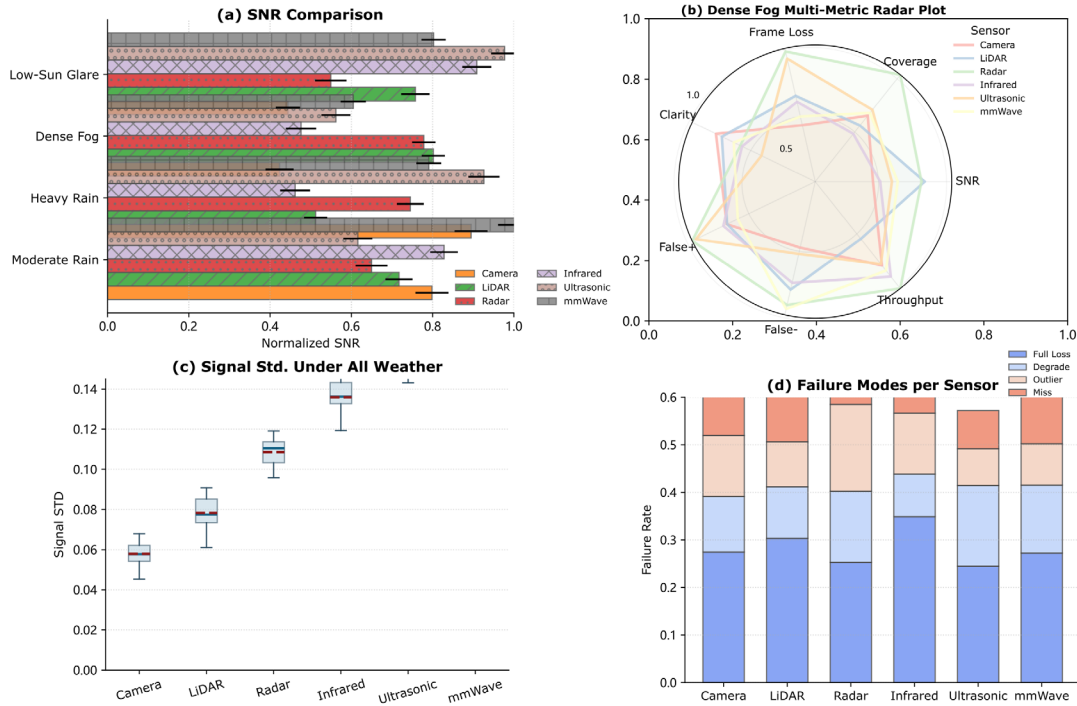


Figure 4. Experimental Scenarios: (a) Moderate Rain, (b) Heavy Rain, (c) Dense Fog, (d) Low-Sun Glare.

Quantitative Results under Adverse Weather

Three quantitative results—perception accuracy, error rate, and a normalised robustness index—are presented under the entire spectrum of unfavourable weather circumstances. The aforementioned findings are displayed in a number of multi-panel images, each of which thoroughly illustrates a different facet of the system's activity.

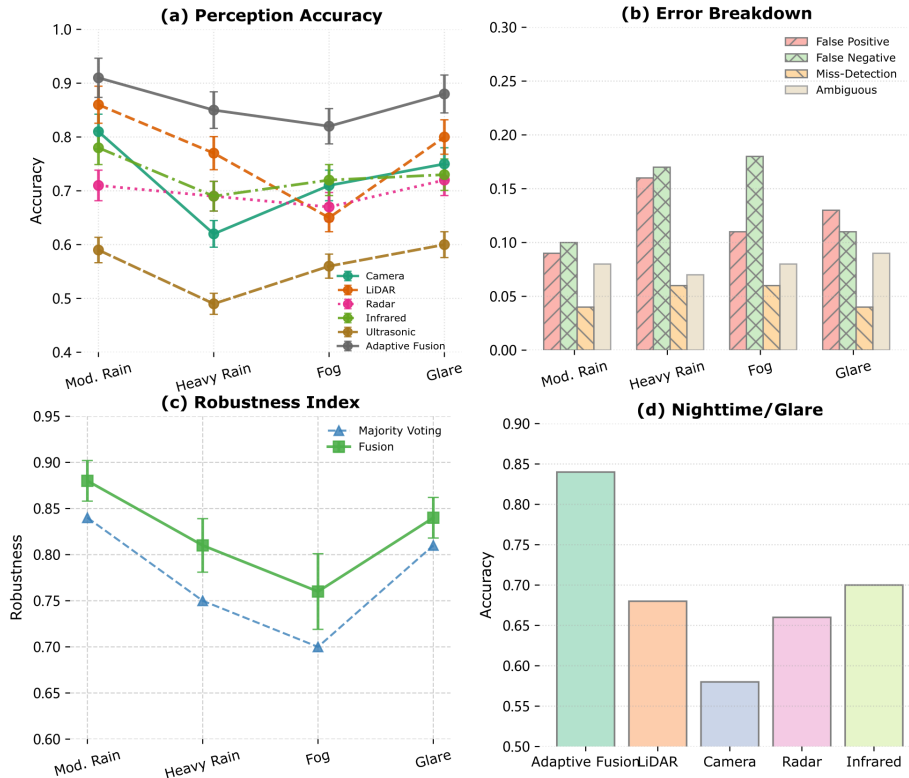


Figure 5. Quantitative Metrics for Major Scenarios: (a) Perception Accuracy, (b) Error Breakdown, (c) Robustness Index, (d) Nighttime/Glare Scenarios.

The results of the two fusion techniques and different sensors are displayed in Figure 5a for all weather situations. When there is mild to moderate to severe rain, camera-only accuracy significantly decreases, but LiDAR and radar are comparatively more reliable. The suggested adaptive fusion has repeatedly demonstrated the best performance and may effectively leverage the advantages of each modality in a variety of situations.

We have also separated the error rate into false positives and false negatives, as seen in Figure 5b. Dense fog and heavy rain are better conditions for adaptive fusion; otherwise, a mistake in a single mode would grow quickly, but a fusion system would lessen this error by reducing the weight assigned to an unreliable source.

The robustness index is displayed in Figure 5c. In a variety of unfavourable weather circumstances, the new algorithm has demonstrated the greatest stability and a comparatively narrow range of fluctuations. Lastly, as Figure 5d illustrates, the lighting condition is either low light or glare; at this point, the adaptive fusion module continues to function normally whereas the regular technique shows a discernible decline in performance.

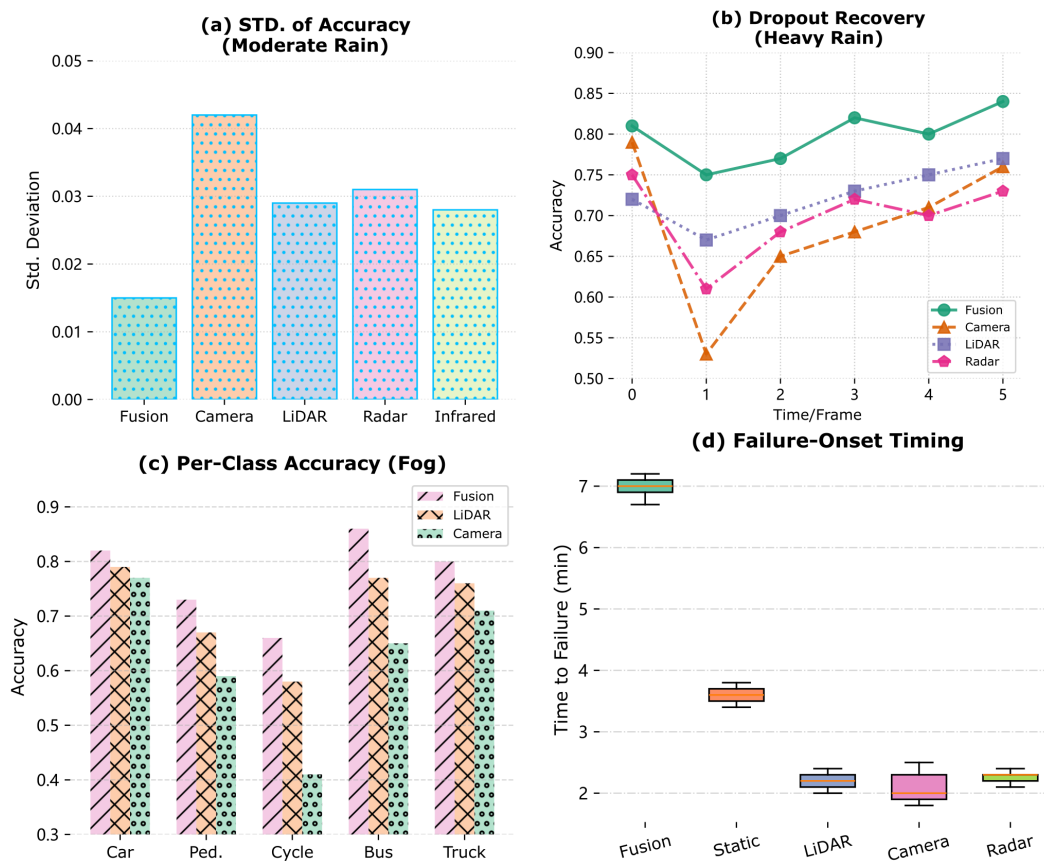


Figure 6. Detailed Performance Analysis: (a) Short-term Robustness, (b) Dropout Recovery, (c) Per-Class Accuracy, (d) Failure-Onset Timing.

The types and reasons of performance variations at various intervals are depicted in Figure 6. The accuracy standard deviation for moderate rain is displayed in Figure 6a. The adaptive system is less erratic than any single-sensor baseline and has strong short-term stability. The algorithm's reaction to a sensor dropout in intense rain is depicted in Figure 6b. Here, our fusion architecture's quick recovery and low accuracy loss contrast sharply with unimodal techniques' steep drops. Cross-class examination of dense fog conditions reveals that only adaptive fusion can sustain multi-class detection performance; otherwise, class bias or degradation occurs, as illustrated in Figure 6c. The mean time to system breakdown under increasing weather influences is shown in Figure 6d. The findings demonstrate that, when compared to single-modality systems under the same stress, our adaptive fusion nearly doubles the safe-operating period.

Ablation Study and Algorithm Comparison

To quantitatively ascertain the individual contributions of the fundamental components in the modified fusion structure, ablation research was conducted. Measure the impact of Bayesian adaptivity, probabilistic reliability weighting, and redundancy mechanisms by selectively disabling their impacts under different adverse weather circumstances. More than 35,000 frames on average for each scenario.

Each module's quantity is displayed in Figure 7. Figure 7a illustrates how the mean perception accuracy under all unfavourable conditions dropped from 81.4% (full model) to 74.1% when Bayesian adaptive weighting was turned off. The accuracy decreased to 68.9% from 77.6% under heavy rain, making it less responsive to real-time weighting for detection. The frequency of outlier selection increased as the scene's complexity increased.

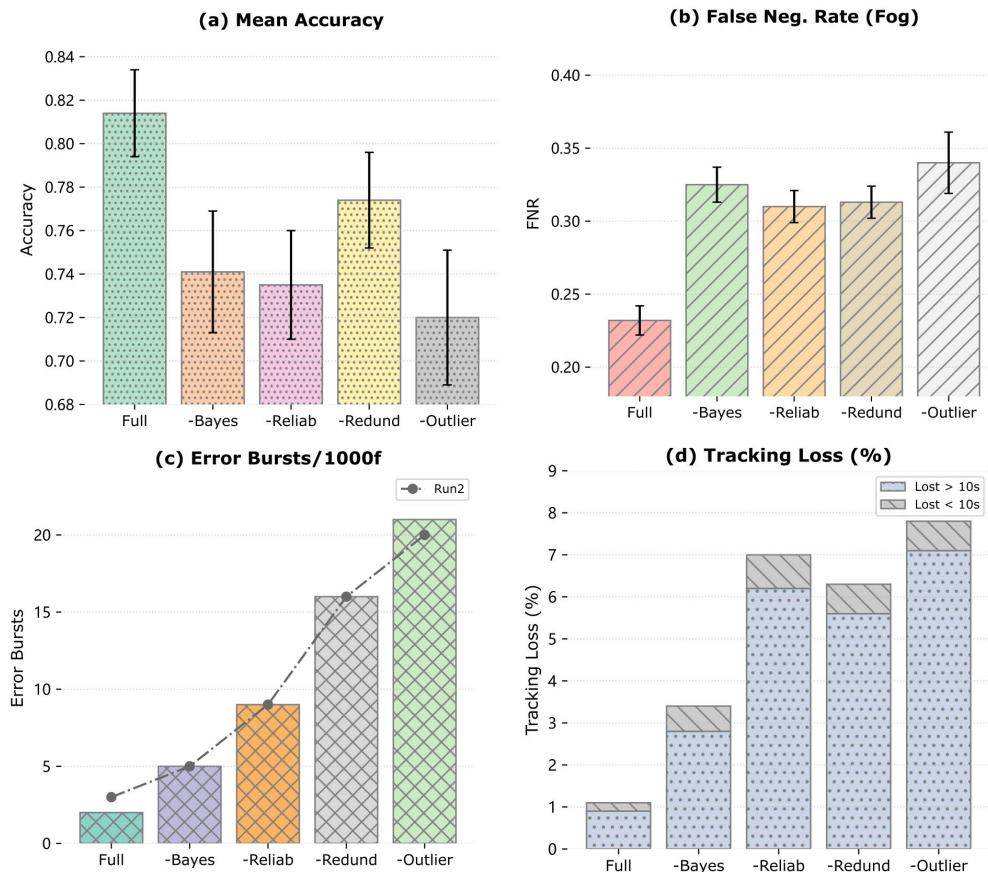


Figure 7. Ablation Study of Module Contribution: (a) Impact of Bayesian Adaptivity, (b) Reliability Estimation Disabled, (c) No Redundancy Handling, (d) All Advanced Modules Disabled.

The average false negative rate increased by 4.7 percentage points when probabilistic reliability estimate was removed, as seen in Figure 7b. This increase was greatest in dense fog (from 23.2% to 32.5%) when compared to the full pipeline. Due to the system's excessive reliance on noisy sensors, numerous non-detections were disregarded in low visibility situations.

Figure 7c shows the results without redundancy management: average error bursts (frame-wise error > 40%) increased from two to sixteen per thousand frames in high-intensity rain sequences, and complete loss of tracking reached 6.2% (versus <1% with redundancy). In practice, these mistake bursts were longer and had an impact on motion estimation as well as obstacle perception.

When all the modules were disabled simultaneously, as shown in Figure 7d, both the accuracy (dropping to 70.3%) and robustness metrics fell to the level of the traditional sensor fusion baseline, and thus the system's main advantage in environmental resistance was lost.

In Figure 8, numerous algorithms were plotted and compared. The suggested approach surpassed deep neural fusion by 6–9%, fixed weighted average by 11–14%, and individual sensors by up to 22%, as seen in Figure 8a. It also attained the highest average accuracy across all meteorological situations. The robustness index (standardised; greater is better) reached 0.88 with the adaptive technique in moderate rain, 0.79 for deep fusion, and as low as 0.71 with LiDAR alone, as shown in Figure 8b.

The adaptive approach still produced a low combined false positive/negative rate of less than 14% in fog, as seen in the full error rate breakdown in Figure 8c. This was far lower than the over 23% reported for either deep or static fusion.

Lastly, as Figure 8d illustrates, the adaptive method's mean time to failure for simulated sensor dropout tests was 6.9 minutes, which was three times longer than any single-modality solution and nearly twice as long as fixed fusion (3.6 minutes).

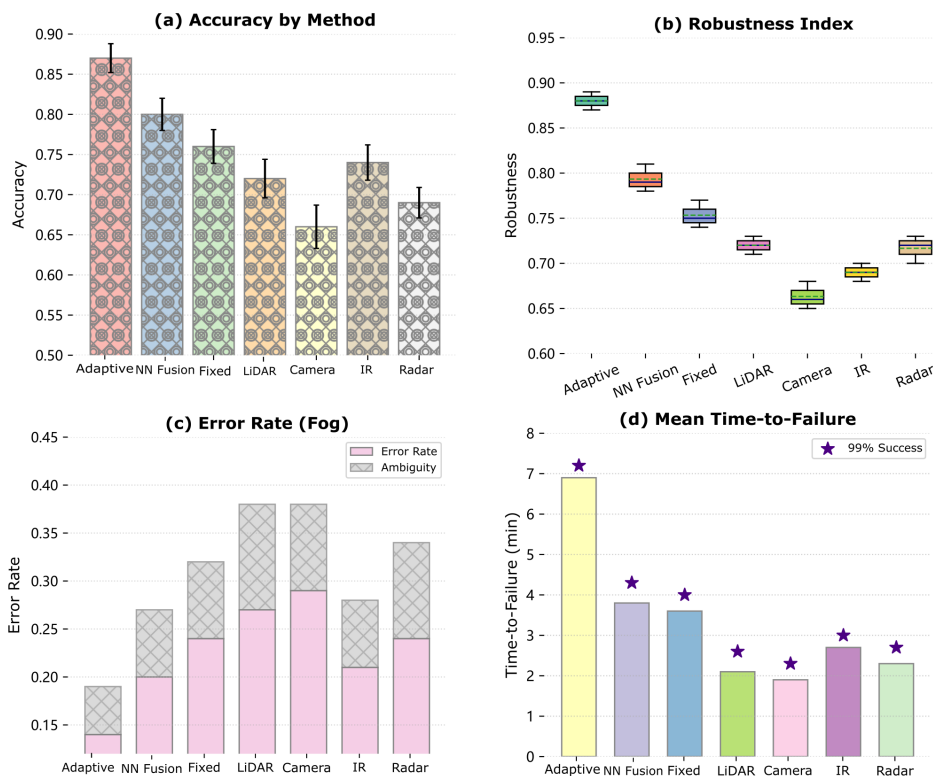


Figure 8. Comparative Analysis with Baseline Fusion Approaches: (a) Accuracy by Method, (b) Robustness Index Across Weather, (c) Error Rate Breakdown, (d) Mean Time-to-Failure.

Discussion and Implications

This study's all-weather autonomous driving scenario has shown that dynamic, uncertainty-aware sensor fusion can be used to improve perceptual robustness. According to the experiment, static fusion weights work well under typical conditions but are readily made erroneous by changes in environmental statistics, such as glare, fog, or rainfall. In line with recent studies on uncertainty-driven perception [26], the adaptive approach described here also has more precision and stability in perception and may distribute confidence in real time based on the sensor's dependability.

The fact that there is now less damage from poor perception during inclement weather is a really positive outcome. Reliable sensor data is dynamically selected from all sources using Bayesian adaptivity and probabilistic reliability estimate, eliminating unreliable data [27]. As a result, the quantity of missed objects and false alarms has been decreased, and a single-modality method is frequently inappropriate on the ground [28].

This framework's redundancy management module is displayed below. The proposed pipeline makes advantage of overlapping sensor fields and temporal consistency proactively to guarantee continuous functioning, whereas

the prior techniques frequently fail when a single sensor drops out or momentarily loses communication [29]. As a result, it will be applied to the creation of a real-time safety perception system.

However, this increase has a negligible processing delay and compute cost. For real-time inference, the adaptive weighting and redundancy modules can operate in parallel on general-purpose car GPU platforms due to their comparatively small size [30]. As a result, the improved robustness will not only exist in theory but will be used as real improvements.

From the standpoint of systems engineering, the safety of system application and regulatory requirements are closely linked to an increase in the robustness index and a decrease in error rates. Recent international standards on automated driving have focused on the system's ability to retain high-confidence detection and fast recovery from failure mode, thereby prolonging the safe fallback window and enhancing overall operational safety [31].

There are still a few unresolved issues and shortcomings, though. Due to a dearth of training data and highly non-stationary noise, the rarest and most extreme weather phenomena, such as sandstorms or hail, remain challenging for any current model [32]. In order to broaden the range of applications, future research will focus on expanding data gathering, augmenting synthetic data, and further integrating self-supervised anomaly detection [33]. New research is currently being done in the fields of novel sensor types and generalisation to unseen domains [34]. Lastly, the concepts of distributed uncertainty modelling discussed here may help create completely cooperative and reliable autonomous vehicle networks as multi-agent and networked perception systems proliferate [35].

Conclusion

This research proposes an adaptive multimodal sensor fusion architecture to improve perceptual robustness for autonomous driving in a variety of challenging and variable weather conditions. The first novel function combines Bayesian adaptation, probabilistic reliability estimate, and redundancy-aware management; it has a great structure that explicitly takes sensor reliability into account and reacts rapidly to environmental changes. This work has achieved reasonably long-term, high-accuracy perception and a high-robustness index that surpasses both static fusion and state-of-the-art neural baselines. This is theoretically consistent with and supports a variety of engineering applications. All of these findings demonstrate that the usefulness of uncertainty-aware perception pipelines for satisfying the requirements of real-world, safety-critical deployment has been confirmed.

There are still some shortcomings. The current approach has not been thoroughly tested in the face of extremely severe or infrequent natural disasters, like hailstorms or dense air pollution; as a result, little training data has been gathered in these scenarios, and unpredictable sensor deterioration renders it unreliable, even though it can handle different types of weather and sensor failures fairly well. Furthermore, there is still room for improvement in the existing model's generalisation to new city layouts, unfamiliar driving scenarios, and different sensor setups. Lastly, computational complexity is very low for the current technology, but it could become a bottleneck when the system size and sensor count grow in the future.

The suggested theoretical and algorithmic foundation will offer a clear path forward for encouraging the growth of robust perception in both academia and business. Future research will focus on developing self-supervised anomaly detection techniques, applying transfer learning methodologies for generalisation, and expanding adaptive fusion to new sensor modules. The aforementioned advancements are anticipated to foster the development of safer, more dependable, and context-aware perception that can function properly in all-weather, multi-domain contexts as the autonomous vehicle ecosystem grows.

Author Contributions

Adrian Dziuba contributes to conceptualization, methodology, software, validation, analysis, investigation, data collection, draft preparation, manuscript editing, visualization, supervision. Henryk Kasprzak and Feliks Karpiński contribute to data collection, draft preparation, manuscript editing. All authors have read and agreed with the manuscript before its submission and publication.

Funding

This research received no specific financial support from any funding agency.

Institutional Review Board Statement

Not applicable.

References

- [1] Zhang, X., Li, Z., Zou, Z., Gao, X., Xiong, Y., Jin, D., ... & Liu, H. (2023). Informative data selection with uncertainty for multimodal object detection. *IEEE Transactions on Neural Networks and Learning Systems*, 35(10), 13561-13573. <https://doi.org/10.1109/TNNLS.2023.3270159>
- [2] Wang, S., Xie, X., Li, M., Wang, M., Yang, J., Li, Z., ... & Zhou, Z. (2024). An Adaptive Multimodal Fusion 3D Object Detection Algorithm for Unmanned Systems in Adverse Weather. *Electronics*, 13(23), 4706. <https://doi.org/10.3390/electronics13234706>
- [3] Senel, N., Kefferpütz, K., Doycheva, K., & Elger, G. (2023). Multi-sensor data fusion for real-time multi-object tracking. *Processes*, 11(2), 501. <https://doi.org/10.3390/pr11020501>
- [4] Sumalatha, I. P. P. A., Chaturvedi, P., Patil, S., Thethi, H. P., & Hameed, A. A. (2024, May). Autonomous multi-sensor fusion techniques for environmental perception in self-driving vehicles. In *2024 International Conference on Communication, Computer Sciences and Engineering (IC3SE)* (pp. 1146-1151). IEEE. <https://doi.org/10.1109/IC3SE62002.2024.10593125>
- [5] Liu, Y., Wang, M., Lasang, P., & Sun, Q. (2023). Importance biased traffic scene segmentation in diverse weather conditions. *IEEE Transactions on Intelligent Vehicles*, 9(1), 2753-2765. <https://doi.org/10.1109/TIV.2023.3272922>
- [6] Berrio, J. S., Shan, M., Worrall, S., & Nebot, E. (2021). Camera-LIDAR integration: Probabilistic sensor fusion for semantic mapping. *IEEE Transactions on Intelligent Transportation Systems*, 23(7), 7637-7652. <https://doi.org/10.1109/TITS.2021.3071647>
- [7] Qin, L., Wang, H., Yuan, Y., & Qin, S. (2021). Multi-sensor perception strategy to enhance autonomy of robotic operation for uncertain peg-in-hole task. *Sensors*, 21(11), 3818. <https://doi.org/10.3390/s21113818>
- [8] Wang, J., Zhang, Z., & Lu, G. (2021). A Bayesian inference based adaptive lane change prediction model. *Transportation research part C: emerging technologies*, 132, 103363. <https://doi.org/10.1016/j.trc.2021.103363>
- [9] Zhang, H., Wu, K., Chen, R., Wu, Z., Zhong, Y., & Li, W. (2024). TL-4DRCF: A two-level 4-D radar-camera fusion method for object detection in adverse weather. *IEEE Sensors Journal*, 24(10), 16408-16418. <https://doi.org/10.1109/JSEN.2024.3382669>
- [10] Xiang, C., Feng, C., Xie, X., Shi, B., Lu, H., Lv, Y., ... & Niu, Z. (2023). Multi-sensor fusion and cooperative perception for autonomous driving: A review. *IEEE Intelligent Transportation Systems Magazine*, 15(5), 36-58. <https://doi.org/10.1109/MITS.2023.3283864>
- [11] Sahoo, S. (2024). Sensor Fusion and Virtual Sensor Design for Enhanced Multi-Sensor Data Accuracy in Autonomous Systems. *International Journal on Smart & Sustainable Intelligent Computing*, 1(2), 21-39. <https://doi.org/10.63503/j.ijssic.2024.31>
- [12] Weng, J., & Xiao, F. (2019). A novel sensor dynamic reliability evaluation method and its application in multi-sensor information fusion. *IEEE Access*, 7, 146144-146157. <https://doi.org/10.1109/ACCESS.2019.2943353>
- [13] Xiao, Y., Liu, Y., Luan, K., Cheng, Y., Chen, X., & Lu, H. (2023). Deep LiDAR-radar-visual fusion for object detection in urban environments. *Remote Sensing*, 15(18), 4433. <https://doi.org/10.3390/rs15184433>
- [14] Wang, K., Zhang, Q., & Hu, X. (2023). Multisensor multitarget tracking arithmetic average fusion method based on probabilistic time window. *IEEE Sensors Journal*, 24(3), 3583-3593. <https://doi.org/10.1109/JSEN.2023.3337267>
- [15] Li, X., & Xu, S. (2021). Multi-sensor complex network data fusion under the condition of uncertainty of coupling occurrence probability. *IEEE Sensors Journal*, 21(22), 24933-24940. <https://doi.org/10.1109/JSEN.2021.3061437>
- [16] Aloufi, N., Alnori, A., & Basuhail, A. (2024). Enhancing autonomous vehicle perception in adverse weather: A multi objectives model for integrated weather classification and object detection. *Electronics*, 13(15), 3063. <https://doi.org/10.3390/electronics13153063>

- [17] Lee, Y., Ko, Y., Kim, Y., & Jeon, M. (2022, May). Perception-friendly video enhancement for autonomous driving under adverse weather conditions. In 2022 International Conference on Robotics and Automation (ICRA) (pp. 7760-7767). IEEE. <https://doi.org/10.1109/ICRA46639.2022.9811870>
- [18] Song, D., Tian, G. M., & Liu, J. (2021, July). Real-time localization measure and perception detection using multi-sensor fusion for Automated Guided Vehicles. In 2021 40th Chinese Control Conference (CCC) (pp. 3219-3224). IEEE. <https://doi.org/10.23919/CCC52363.2021.9550235>
- [19] Wang, K., Wang, Y., Liu, B., & Chen, J. (2023). Quantification of uncertainty and its applications to complex domain for autonomous vehicles perception system. *IEEE Transactions on Instrumentation and Measurement*, 72, 1-17. <https://doi.org/10.1109/TIM.2023.3256459>
- [20] Ur Rehman, M., Jamshed, M. A., & Kalsoom, T. (2024). Advances in Multi-modal Intelligent Sensing. *Multimodal Intelligent Sensing in Modern Applications*, 1-28. <https://doi.org/10.1002/9781394257744.ch1>
- [21] Zhu, H., Wang, Q., Li, Y., & Leung, H. (2022). Variational Bayesian based localization for intelligent vehicle using lidar and GPS data fusion: Algorithm and experiments. *IEEE/ASME Transactions on Mechatronics*, 27(6), 5659-5667. <https://doi.org/10.1109/TMECH.2022.3187975>
- [22] Cheng, L., Zang, H., Ding, T., Wei, Z., & Sun, G. (2021). Multi-meteorological-factor-based graph modeling for photovoltaic power forecasting. *IEEE Transactions on Sustainable Energy*, 12(3), 1593-1603. <https://doi.org/10.1109/TSTE.2021.3057521>
- [23] Qiu, M., Bazan, P., Antesberger, T., Bock, F., & German, R. (2021, December). Reliability assessment of multi-sensor perception system in automated driving functions. In 2021 IEEE 26th Pacific Rim International Symposium on Dependable Computing (PRDC) (pp. 104-112). IEEE. <https://doi.org/10.1109/PRDC53464.2021.00022>
- [24] Grewal, R., Tonella, P., & Stocco, A. (2024, May). Predicting safety misbehaviours in autonomous driving systems using uncertainty quantification. In 2024 IEEE Conference on Software Testing, Verification and Validation (ICST) (pp. 70-81). IEEE. <https://doi.org/10.1109/ICST60714.2024.00016>
- [25] Zhang, C., Wang, H., Cai, Y., Chen, L., & Li, Y. (2024). TransFusion: multi-modal robust fusion for 3D object detection in foggy weather based on spatial vision transformer. *IEEE Transactions on Intelligent Transportation Systems*, 25(9), 10652-10666. <https://doi.org/10.1109/TITS.2024.3420432>
- [26] Mohammed, A. S., Amamou, A., Ayevide, F. K., Kelouwani, S., Agbossou, K., & Zioui, N. (2020). The perception system of intelligent ground vehicles in all weather conditions: A systematic literature review. *Sensors*, 20(22), 6532. <https://doi.org/10.3390/s20226532>
- [27] Singh, P., & Singh, L. K. (2021). Improved measurement accuracy in critical parameters of safety-critical systems with multisensor data fusion. *IEEE Transactions on Instrumentation and Measurement*, 70, 1-8. <https://doi.org/10.1109/TIM.2021.3124852>
- [28] Yeong, D. J., Velasco-Hernandez, G., Barry, J., & Walsh, J. (2021). Sensor and sensor fusion technology in autonomous vehicles: A review. *Sensors*, 21(6), 2140. <https://doi.org/10.3390/s21062140>
- [29] Dewangan, V., Sharma, B., Choudhary, T., Sharma, S., Aanegola, A., Singh, A. K., & Krishna, K. M. (2023, August). UAP-BEV: Uncertainty aware planning using bird's eye view generated from surround monocular images. In 2023 IEEE 19th International Conference on Automation Science and Engineering (CASE) (pp. 1-8). IEEE. <https://doi.org/10.1109/CASE56687.2023.10260358>
- [30] Antonakaki, A., Oikonomou, M. G., Garefalakis, T., & Yannis, G. (2024). Driving automation systems penetration and traffic safety: Implications for infrastructure design and policy. *Infrastructures*, 9(12), 234. <https://doi.org/10.3390/infrastructures9120234>
- [31] Wu, W., Deng, X., Jiang, P., Wan, S., & Guo, Y. (2023). CrossFuser: Multi-modal feature fusion for end-to-end autonomous driving under unseen weather conditions. *IEEE Transactions on Intelligent Transportation Systems*, 24(12), 14378-14392. <https://doi.org/10.1109/TITS.2023.3307589>
- [32] Li, Q., Zhuang, Y., Huai, J., Wang, X., Wang, B., & Cao, Y. (2024). A robust data-model dual-driven fusion with uncertainty estimation for LiDAR-IMU localization system. *ISPRS Journal of Photogrammetry and Remote Sensing*, 210, 128-140. <https://doi.org/10.1016/j.isprsjprs.2024.03.008>
- [33] Yi, W., & Chai, L. (2021). Heterogeneous multi-sensor fusion with random finite set multi-object densities. *IEEE Transactions on Signal Processing*, 69, 3399-3414. [10.1109/TSP.2021.3087033](https://doi.org/10.1109/TSP.2021.3087033)
- [34] Zhang, W. A., Fu, R., & Yang, X. (2024). A unified gaussian filtering fusion approach for multisensor uncertain systems. *IEEE Transactions on Aerospace and Electronic Systems*, 60(5), 6376-6384. <https://doi.org/10.1109/TAES.2024.3405903>

- [35] Butt, F. A., Chattha, J. N., Ahmad, J., Zia, M. U., Rizwan, M., & Naqvi, I. H. (2022). On the integration of enabling wireless technologies and sensor fusion for next-generation connected and autonomous vehicles. *IEEE access*, 10, 14643-14668. <https://doi.org/10.1109/ACCESS.2022.3145972>